

# Vanadium Oxide Foams: An Insight into the Structure of the Vanadium Oxide Walls

Olivier Durupthy,<sup>\*,†</sup> Maguy Jaber,<sup>‡</sup> Nathalie Steunou,<sup>\*,†</sup> Jocelyne Maquet,<sup>†</sup>  
G. T. Chandrappa,<sup>§</sup> and Jacques Livage<sup>†</sup>

Laboratoire de Chimie de la Matière Condensée, UMR CNRS 7574, Université Paris VI,  
4 Place Jussieu, 75252 Paris Cedex 05, France, Laboratoire de Matériaux à Porosité Contrôlée,  
UMR CNRS 7016, Université de Haute Alsace, 3 rue Alfred Werner, 68093 Mulhouse Cedex, France,  
and Department of Chemistry, Bangalore University, Bangalore-560 012, India

Received July 1, 2005. Revised Manuscript Received September 28, 2005

Vanadium oxide foams have been prepared by mixing V<sub>2</sub>O<sub>5</sub> with hydrogen peroxide and a solution of 1-hexadecylamine. The resulting yellow foams (YF) have been characterized by different methods including X-ray diffraction, thermal analyses, scanning and transmission electron microscopy, infrared spectroscopy, electron spin resonance, and <sup>51</sup>V MAS NMR spectroscopy. The local environment of vanadium probed by <sup>51</sup>V MAS NMR consists of tetrahedral and octahedral vanadium sites corresponding to the decavanadate [H<sub>x</sub>V<sub>10</sub>O<sub>28</sub>]<sup>(6-x)-</sup> and [V<sub>4</sub>O<sub>10</sub>]<sup>4-</sup>/[V<sub>2</sub>O<sub>7</sub>]<sup>4-</sup> polyanions. This composition is in fair agreement with the reactivity of YF under acidic or basic conditions. Finally, a model for the YF structure based on amine layers intercalated with [H<sub>x</sub>V<sub>10</sub>O<sub>28</sub>]<sup>(6-x)-</sup> and [V<sub>4</sub>O<sub>10</sub>]<sup>4-</sup>/[V<sub>2</sub>O<sub>7</sub>]<sup>4-</sup> polyanions is proposed.

## Introduction

Hybrid organic–inorganic materials based on vanadium oxide have received significant attention due to their ionic and electronic properties leading to potential applications in various domains such as reversible cathodes for lithium batteries, electrochromic devices, or heterogeneous catalysis.<sup>1–4</sup> Numerous vanadium oxide compounds exhibit a layered structure allowing the intercalation of a wide range of organic molecules.<sup>5–9</sup> In an attempt to design materials with a multiscale porosity, various physical and chemical methods have been developed that include gas bubbling in a reacting medium, phase segregation, and microemulsions.<sup>10–12</sup> Macroporous oxide materials with pores larger than 50 nm could be interesting for application as catalytic surfaces, adsorbents, chromatographic materials, filters, lightweight structural

materials, and thermal, acoustic, and electrical insulators.<sup>13–15</sup> In this context, macroporous vanadium oxide foams were prepared mainly by two different routes. Recently, macroporous V<sub>2</sub>O<sub>5</sub> foams were prepared by bubbling perfluorohexane gas produced in situ through a viscous, already formed, vanadium oxide gel.<sup>16</sup> This strategy based on bubbling air–liquid foaming systems allows a high control over the vanadium oxide cell morphologies (length, width, and curvature of the Plateau borders). Three years ago, an easier chemical process based on the in-situ dissociation of hydrogen peroxide with V<sub>2</sub>O<sub>5</sub> in the presence of surfactant was reported.<sup>17</sup> The vanadium oxide foams were actually not amorphous and exhibit lamellar ordering as indicated by *00l* reflections in a typical XRD pattern of the foam.<sup>17</sup> However, this method leads to a structural disorder in terms of the porosity (pores diameter, walls thickness) and of the vanadium oxide network. Therefore, the limited diffraction pattern with no sharp Bragg peaks makes impossible the determination of the 3D crystallographic structure. This paper presents an analysis of the structure of these foams using of several complementary techniques such as X-ray diffraction, thermal analyses, scanning, and transmission electron microscopy. <sup>51</sup>V MAS NMR spectroscopy (including modeling of the spectra) was used to identify vanadium environments constituting the walls. Indeed, different vanadium species can be distinguished and characterized by the determination of the <sup>51</sup>V chemical shift anisotropy (CSA) and the quadrupole coupling parameters that are related to the structural parameters such as vanadium coordination and the degree

\* Address correspondence to either author. Phone: (0033)-1-44-27-55-45. Fax: (0033)-1-44-27-47-69. E-mail: steunou@ccr.jussieu.fr (N.S.); durupthy@ccr.jussieu.fr (O.D.).

<sup>†</sup> Université Paris VI.

<sup>‡</sup> Université de Haute Alsace.

<sup>§</sup> Bangalore University.

- (1) Nabavi, M.; Doeuff, S.; Sanchez, C.; Livage, J. *Mater. Sci. Eng.* **1989**, *B3*, 203.
- (2) Livage, J. *Catal. Today* **1998**, *41*, 3.
- (3) Hibino, M.; Ugaji, M.; Kishimoto, A.; Kudo, T. *Solid State Ionics* **1995**, *79*, 239.
- (4) Jouanneau, S.; Le Gal La Salle, A.; Verbaere, A.; Deschamps, M.; Lascaud, S.; Guyomard, D. *J. Mater. Chem.* **2003**, *13*, 921.
- (5) Livage, J. *Chem. Mater.* **1991**, *3*, 578.
- (6) Li, Z. F.; Ruckenstein, E. *Langmuir* **2002**, *18*, 6956.
- (7) Kuwabata, S.; Masui, S.; Tomiyori, H.; Yoneyama, H. *Electrochim. Acta* **2000**, *46*, 91.
- (8) Huguenin, F.; Torresi, R. M.; Buttry, D. A. *J. Electrochem. Soc.* **2002**, *149*, A546.
- (9) Wu, C. G.; DeGroot, D. C.; Marcy, H. O.; Schindler, J. L.; Kannewurf, C. R.; Liu, Y. J.; Hirpo, W.; Kanatzidis, M. G. *Chem. Mater.* **1996**, *8*, 1992.
- (10) Mann, S. *Angew. Chem., Int. Ed.* **2000**, *39*, 3392.
- (11) Iwasaki, M.; Davis, S. A.; Mann, S. *J. Sol–Gel Sci. Technol.* **2004**, *32*, 99.
- (12) Mann, S.; Ozin, G. A. *Nature* **1996**, *382*, 313.

(13) Rolison, D. R.; Dunn, B. *J. Mater. Chem.* **2001**, *11*, 963.

(14) Ayen, R. J.; Iacobucci, P. A. *Rev. Chem. Eng.* **1988**, *5*, 157.

(15) Pajonk, G. M. *Appl. Catal.* **1991**, *72*, 217.

(16) Carn, F.; Steunou, N.; Livage, J.; Colin, A.; Backov, R. *Chem. Mater.* **2005**, *17*, 644.

(17) Chandrappa, G. T.; Steunou, N.; Livage, J. *Nature* **2002**, *416*, 702.

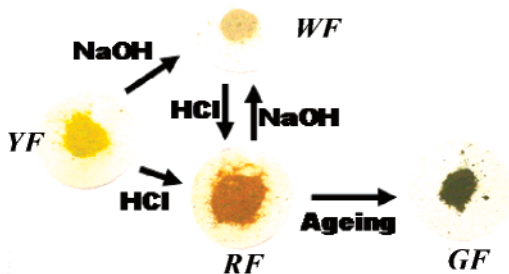


**Figure 1.** Photographs of the foams (YF = yellow foam, WF = white foam, RF = red foam, GF = green foam). WF, RF, and GF compounds were obtained after the exposure of the YF to  $\text{NH}_3$  or HCl vapors.

of polymerization of  $\text{VO}_n$  units.<sup>18–25</sup> This paper deals also with the chemical reactivity of the foam in the presence of  $\text{NH}_3$  and HCl gas. The resulting modified foams have been characterized by NMR spectroscopy. Finally, a structure of the vanadium oxide foams is proposed.

### Experimental Section

**Synthesis.** Vanadium oxide foams were synthesized according to the already described procedure.<sup>17</sup> The yellow foams (YF) were obtained by mixing vanadium oxide powder ( $\text{V}_2\text{O}_5$ , Prolabo 99.5%, 1 g, 5.5 mmol) with a solution of 1-hexadecylamine (Aldrich 98%,  $\text{C}_{16}\text{H}_{33}\text{NH}_2$ , 1.33 g, 5.5 mmol) in 3 mL of acetone. A paste-like material was formed to which an aqueous solution of hydrogen peroxide ( $\text{H}_2\text{O}_2$ , Prolabo, 50 mL, 30% in wt) was added. The exothermic decomposition of  $\text{H}_2\text{O}_2$  leads to the in-situ formation of oxygen gas, and a voluminous YF forms spontaneously within few minutes. The pH of the reacting solution was around 2, and the temperature was close to 60 °C. The foam was then separated from the solution and dried in air during 16 h. This YF appears to be highly reactive as described below and summarized in Figure 1. YFs were put under vapors of aqueous ammonia (20% in weight) in a closed vessel. Under these basic conditions, YFs evolved into white ones (WF) within a few minutes. Those WFs were stable with time even when left in air. In the presence of HCl vapors, YFs rapidly turn red. These red foams (RF) were not stable in air and became green foams (GF) within a few hours. WFs could be reversibly converted into RFs by pouring them alternatively in acidic and basic vapors. However GFs could not turn white with  $\text{NH}_3$ .

$\text{Cs}_4[\text{H}_2\text{V}_{10}\text{O}_{28}]\cdot 4\text{H}_2\text{O}$  was synthesized as a reference compound in order to characterize the vanadium oxide foams by  $^{51}\text{V}$  solid-state NMR. This cesium dihydrogenodecavanadate was prepared by the acidification of an aqueous solution of sodium metavanadate  $\text{NaVO}_3$  (Sigma, >99%,  $0.5 \text{ mol}\cdot\text{L}^{-1}$ , pH = 8) using a proton exchange resin (Dowex 50WX 4-100 mesh). A clear yellow solution (pH = 1) was obtained after full proton exchange. Small volumes of CsOH solutions ( $2 \text{ mol}\cdot\text{L}^{-1}$ ) were added in order to set the pH

of the solution to 3. The orange precipitate formed immediately was separated from the supernatant solution, rinsed twice with 20 mL of deionized water, and left to dry 24 h at room temperature. The structure of this compound was identified by powder X-ray diffraction. The X-ray diffraction pattern was found identical to the one calculated from the previously reported single-crystal X-ray data.<sup>26</sup> The molar ratio Cs/V = 0.4 of this compound was confirmed by chemical analysis.

**Characterization.** X-ray powder diffraction patterns were recorded on a Philips PW 1830 diffractometer using Cu  $K\alpha$  radiation ( $\lambda = 1.542 \text{ \AA}$ ). Scanning electron microscopy (SEM) studies were performed on a Cambridge stereoscan 120 microscope using gold-coated samples. Transmission electron microscopy (TEM) investigations were carried out on a JEOL 100 CX II microscope. One droplet of the powder dispersed in  $\text{CHCl}_3$  was deposited onto a carbon-coated copper grid and left to dry in air. Foams were characterized by FTIR spectroscopy using a Nicolet Magna-IRTM spectrometer 750. Thermogravimetric analyses (TGA) were performed on a TA SDT 2960 apparatus. Foams were heated to 600 °C with a heating rate of  $5 \text{ }^\circ\text{C}\cdot\text{min}^{-1}$  in an oxygen atmosphere. Solid-state  $^{51}\text{V}$  MAS NMR spectra were recorded at 79.0 MHz on a Bruker Avance 300 spectrometer using a MQ-MAS 4 mm probe in order to shorten pulse length. Solid samples were spun both at 10 and 14 kHz using  $\text{ZrO}_2$  rotors.  $^{51}\text{V}$  MAS NMR spectra were acquired with a Hahn echo sequence ( $\theta-\tau-2\theta-\tau$  acquisition) with a synchronized  $\tau$  (with the rotor frequency) and a 16 phases pulse program. The following acquisition parameters were used: spectral width of 1 MHz, pulse width of  $\theta = 0.7 \mu\text{s}$  ( $t_{\pi/2} \text{ }^{51}\text{V liq} = 2.5 \mu\text{s}$ ) and 0.5 s of recycle time. An accumulation of 14 000 transients was usually performed on each sample. Isotropic chemical shifts were reported to pure  $\text{VOCl}_3$  using a solution of  $0.1 \text{ mol}\cdot\text{L}^{-1} \text{ NH}_4\text{VO}_3$  ( $\delta_{\text{iso}} = -578 \text{ ppm}$ ) as secondary reference. Numerical simulations of the  $^{51}\text{V}$  MAS spectra were performed with the dmfit-QUASAR program.<sup>27</sup> These simulations included the effects of the chemical shift anisotropy CSA as well as first- and second-order quadrupolar interactions; both central and satellite transitions were considered. Several line-shape parameters describing these interactions have been determined, including the quadrupole coupling constant ( $C_Q$ ), the asymmetry parameter ( $\eta_Q$ ), the isotropic chemical shift ( $\delta_{\text{iso}}$ ), the CSA ( $\Delta\delta_{\text{CSA}}$ ), and the CSA asymmetry parameter ( $\eta_{\text{CSA}}$ ). Chemical shift tensor parameters  $\delta_{\text{iso}}$ ,  $\Delta\delta_{\text{CSA}}$ , and  $\eta_{\text{CSA}}$  are defined as  $\delta_{\text{iso}} = (\delta_{11} + \delta_{22} + \delta_{33})/3$ ,  $\Delta\delta_{\text{CSA}} = (\delta_{33} - \delta_{\text{iso}})$ , and  $\eta_{\text{CSA}} = (\delta_{22} - \delta_{11})/(\delta_{33} - \delta_{\text{iso}})$ . The Euler angles ( $\varphi$ ,  $\chi$ , and  $\psi$ ) between CSA and quadrupolar tensors could not be correctly estimated because of the low values of the CSA parameters. X-band ESR investigations were recorded with a Bruker ESP 300E spectrometer at ca. 9.24 GHz at both 298 and 77 K. ESR parameters were obtained using the program SIMFONIA.<sup>28</sup>

### Results and Discussion

**Nature of the YF.** YFs are highly porous materials as shown by the production of 3 L of foam from only 1 g of  $\text{V}_2\text{O}_5$  dispersed in 50 mL of aqueous solution. During the drying time, a slight break of the foam is observed. As shown previously by SEM,<sup>17</sup> large pores, a few micrometers in diameter, are polydisperse in size and are surrounded by thick walls of about  $1 \mu\text{m}$  (see Figure 2).

- (18) Lapina, O. B.; Shubin, A. A.; Khabibulin, D. F.; Terskikh, V. V.; Bodart, P. R.; Amoureux, J.-P. *Catal. Today* **2003**, *78*, 91.  
 (19) Skibsted, J.; Jacobsen, C. J. H.; Jakobsen, H. J. *Inorg. Chem.* **1998**, *37*, 3083.  
 (20) Hayakawa, S.; Yoko, T.; Sakka, S. *Bull. Chem. Soc. Jpn.* **1993**, *66*, 3393.  
 (21) Hayakawa, S.; Yoko, T.; Sakka, S. *J. Solid State Chem.* **1994**, *112*, 329.  
 (22) Skibsted, J.; Nielsen, N. C.; Bildsoe, H.; Jakobsen, H. J. *J. Am. Chem. Soc.* **1993**, *115*, 7351.  
 (23) Nielsen, U. G.; Jakobsen, H. J.; Skibsted, J. *J. Phys. Chem. B* **2001**, *105*, 420.  
 (24) Fontenot, C. J.; Wiench, J. W.; Pruski, M.; Schrader, G. L. *J. Phys. Chem. B* **2001**, *105*, 10496.  
 (25) Nielsen, U. G.; Jakobsen, H. J.; Skibsted, J. *Inorg. Chem.* **2000**, *39*, 2135.

- (26) Rigotti, G.; Rivero, B. E.; Castellano, E. E. *Acta Crystallogr., Sect. C: Cryst. Struct. Commun.* **1987**, *43*, 197.  
 (27) Massiot, D.; Fayon, F.; Capron, M.; King, I.; Le Calvé, S.; Alonso, B.; Durand, J.-O.; Bujoli, B.; Gan, Z.; Hoatson, G. *Magn. Reson. Chem.* **2002**, *40*, 70.  
 (28) Bruker-Biospin. *SimFonia: EPR Data Analysis and Simulation*; 2004.

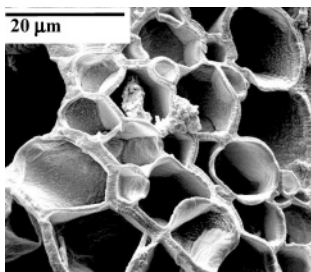


Figure 2. SEM micrograph of the yellow foam (YF).

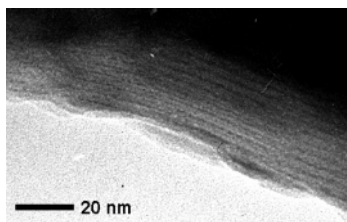


Figure 3. TEM micrograph of the yellow foam (YF).

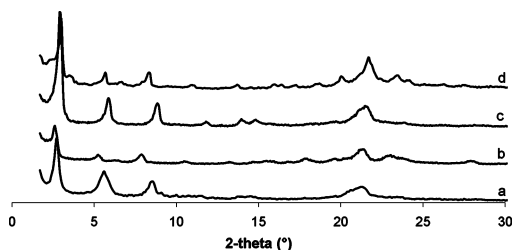


Figure 4. X-ray diffraction pattern of (a) YF, (b) WF, (c) RF, and (d) GF.

TEM micrographs of the YF show a layered structure of the walls with alternative dark and bright fringes with a repetition length of 3.3 nm (Figure 3). The X-ray diffraction pattern (Figure 4a) displays three peaks at low scattering angles assigned to the  $00l$  series of reflection typical of a layered structure. The basal distance  $d_{001} = 3.3$  nm indicates that hexadecylamine molecules are intercalated between the vanadium oxide layers. Taking into account this basal distance and the length of the hexadecylamine ( $\sim 2.2$  nm), different arrangements of the amines in the interlayer space are possible. The hexadecylamine molecules may be packed into a monolayer with amine molecules perpendicular to the vanadium oxide sheets or into a double layer with a tilt angle.<sup>29–31</sup>

Thermogravimetric analyses show that the YFs contain almost no water. A large weight loss is observed between 200 and 400 °C corresponding to the combustion of hexadecylamine molecules (65% in weight). The last 35% in weight corresponds to vanadium oxide. YFs were found to be hydrophobic. They cannot be dispersed into water and remain at the surface of an aqueous solution. This is consistent with the presence of a large amount of long alkyl chains in the solid and at its surface as confirmed by IR spectroscopy. The IR spectrum of the YF displays bands in the 2960–2847 and 1470–1390  $\text{cm}^{-1}$  regions that are assigned to the  $\nu(\text{C}-\text{H})$  and  $\delta(\text{C}-\text{H})$  vibrations, respectively.

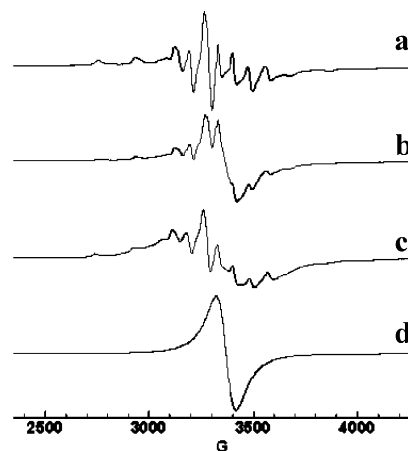


Figure 5. ESR spectra of (a) WF, (b) YF, (c) RF, and (d) GF at 77 K.

The broad band centered at 3200  $\text{cm}^{-1}$  can be assigned to the stretching band  $\nu(\text{N}-\text{H})$  of the  $\text{NH}_2$  group. The spectrum of the pure hexadecylamine shows a strong band at 3335  $\text{cm}^{-1}$  and a weaker one at 3260  $\text{cm}^{-1}$  due to the asymmetric and the symmetric stretching of the  $\text{NH}_2$  group.<sup>32</sup> The  $\text{NH}_2$  deformation band is observed in the YFs foams at 1605  $\text{cm}^{-1}$  (1613  $\text{cm}^{-1}$  in pure hexadecylamine). These shifts of the  $\text{NH}_2$  frequency with respect to that of  $\text{C}_{16}\text{H}_{33}\text{NH}_2$  could be due to the interaction of  $\text{NH}_2$  groups with the inorganic matrix. The 1050–400  $\text{cm}^{-1}$  region that corresponds mainly to vibrations of inorganic compounds is quite similar to that of a hexadecylamine–decavanadate mixture. In particular, the two vibration bands at 958 and 920  $\text{cm}^{-1}$  assigned to the  $\nu(\text{V}=\text{O})$  vibration of vanadyl groups are observed in the spectra of YF and decavanadate.<sup>33,34</sup> Both IR spectra display also a vibration band at 640  $\text{cm}^{-1}$  corresponding to the  $\nu(\text{V}_2\text{O})$  vibration of the vanadium oxide network.

Despite their color yellow foams contain a small amount of reduced  $\text{V}^{\text{IV}}$  ions as shown by ESR experiments. The ESR spectrum of YF (Figure 5b) exhibits the typical hyperfine structure of the vanadyl  $\text{V}^{4+}$  ions ( $S = 1/2$ ,  $I = 7/2$ ) in an axially distorted crystal field. It can be described by the usual spin Hamiltonian:  $H = g_{\parallel}\beta\text{H}_zS_z + g_{\perp}\beta(\text{H}_xS_x + \text{H}_yS_y) + A_{\parallel}S_zI_z + A_{\perp}(S_xI_x + S_yI_y)$  where the parallel direction “z” corresponds to the short  $\text{V}=\text{O}$  bond. The parallel features measured on the spectrum are  $g_{\parallel} = 1.93$  and  $A_{\parallel} = 190$  G (width = 25 G); the perpendicular features simulated from the spectrum are  $g_{\perp} = 1.99$  and  $A_{\perp} = 65$  G (width = 55 G). Both spectra recorded at 77 and 300 K are very similar showing that unpaired electrons remain localized on  $\text{V}^{4+}$  sites analogous to hydrated  $[\text{VO}(\text{H}_2\text{O})_5]^{2+}$  species.<sup>5,35</sup> As most vanadium centers exist mainly in the  $\text{V}(\text{V})$  oxidation state, solid-state  $^{51}\text{V}$  NMR should be suitable to probe the local environment of vanadium in the solid. Three samples of YF obtained from an equivalent synthesis procedure were characterized by  $^{51}\text{V}$  MAS NMR spectroscopy. The  $^{51}\text{V}$  MAS

(29) Krumeich, F.; Muhr, H.-J.; Niederberger, M.; Bieri, F.; Schnyder, B.; Nesper, R. *J. Am. Chem. Soc.* **1999**, *121*, 8324.

(30) Bouhaouss, A.; Aldebert, P. *Mater. Res. Bull.* **1983**, *18*, 1247.

(31) Mizuno, N.; Hatayama, H.; Uchida, S.; Taguchi, A. *Chem. Mater.* **2001**, *13*, 179.

(32) Silverstein, R. M.; Bassler, G. C.; Morrill, T. C. *Spectrometric Identification of Organic Compounds*, 5th ed.; John Wiley and Sons: New York, 1991.

(33) Nakamura, S.; Ozeki, T. *J. Chem. Soc., Dalton Trans.* **2001**, 472.

(34) Wery, A. S. J.; Gutierrez-Zorrilla, J. M.; Luque, A.; Roman, P. *Polyhedron* **1996**, *15*, 4555.

(35) Goodman, B. A.; Raynor, J. B. *Adv. Inorg. Chem. Radiochem.* **1970**, *13*, 135.

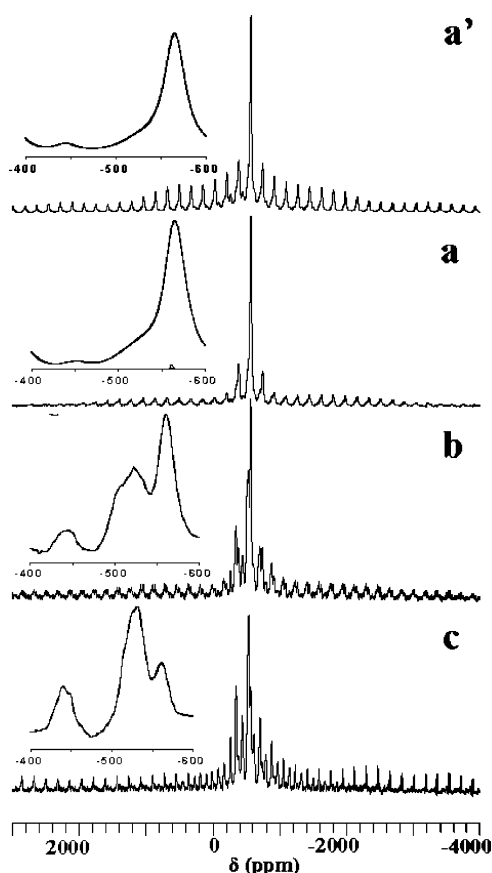


**Figure 6.** (a)  $^{51}\text{V}$  MAS NMR spectrum of one yellow foam sample and (a') the corresponding simulation performed with QUASAR. (b and c)  $^{51}\text{V}$  MAS NMR spectra of two samples of YF. The isotropic part of the spectra is enlarged in the insets.

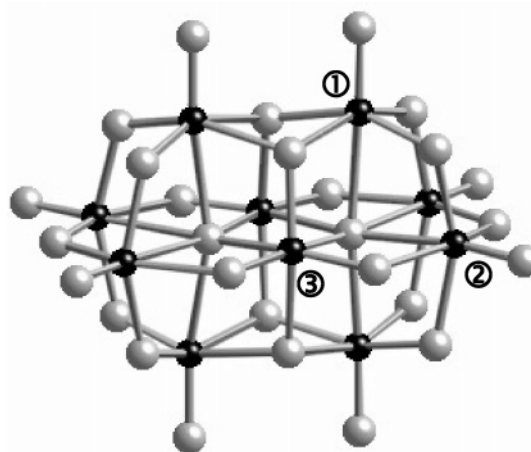
**Table 1. Isotropic Chemical Shift ( $\delta_{\text{iso}}$ ), Quadrupole Coupling Constant ( $C_Q$ ), Quadrupolar Asymmetry Parameter ( $\eta_Q$ ), Chemical Shift Anisotropy ( $\Delta\delta_{\text{CSA}}$ ), and CSA Asymmetry Parameter ( $\eta_{\text{CSA}}$ ) Obtained by QUASAR Simulations<sup>a</sup> of  $^{51}\text{V}$  MAS NMR Spectra**

samples	sites	$\delta_{\text{iso}}$ (ppm) <sup>b</sup>	$C_Q$ (kHz)	$\eta_Q$	$\Delta\delta_{\text{CSA}}$ (ppm) <sup>b</sup>	$\eta_{\text{CSA}}^b$
YF	1	-435	3900	0.3	-400	0.2
	2	-530	3000	0.9	-350	0.2
	3	-564	2000	1.0	-140	0.2
WF	1	-564	2000	1.0	-100	0.2
	2	-578	2500	0.7	-200	0.3
GF	1	-525	3000	0.9	-350	0.5
$\text{Cs}_4[\text{H}_2\text{V}_{10}\text{O}_{28}]\cdot 4\text{H}_2\text{O}$	1	-518	3000	0.9	-400	0.2
	2	-531	2500	0.7	-600	0.7
	3	-540	2500	0.9	-450	0.5
	4	-545	4000	0.5	-450	0.2
$\text{NaV}_3\text{O}_8\cdot 1.5\text{H}_2\text{O}^c$	$\text{V}_a$	-427	6400	0.4	-350	0.2
	$\text{V}_b$	-548	3100	0.9	-420	0
		-535	2400	0.8	-370	0

<sup>a</sup> The data were obtained with the following accuracy:  $C_Q \pm 200$  kHz;  $\eta_Q$  and  $\eta_{\text{CSA}} \pm 0.2$ ;  $\delta_{\text{iso}} \pm 2$  ppm; ( $\varphi$ ,  $\chi$ ,  $\psi$ ) close to (0, 60, 0) values, respectively, for the vanadium sites of the different foams.  $C_Q \pm 100$  kHz;  $\eta_Q$  and  $\eta_{\text{CSA}} \pm 0.1$ ;  $\delta_{\text{iso}} \pm 1$  ppm; ( $\varphi$ ,  $\chi$ ,  $\psi$ ) close to (0, 0, 0) values, respectively, for the vanadium sites of  $\text{Cs}_4[\text{H}_2\text{V}_{10}\text{O}_{28}]\cdot 4\text{H}_2\text{O}$ . <sup>b</sup> Chemical shift tensor parameters  $\delta_{\text{iso}}$ ,  $\Delta\delta_{\text{CSA}}$ , and  $\eta_{\text{CSA}}$  are defined as  $\delta_{\text{iso}} = (\delta_{11} + \delta_{22} + \delta_{33})/3$ ,  $\Delta\delta_{\text{CSA}} = (\delta_{33} - \delta_{\text{iso}})$  and  $\eta_{\text{CSA}} = (\delta_{22} - \delta_{11})/(\delta_{33} - \delta_{\text{iso}})$ . <sup>c</sup> Data taken from ref 38.

NMR spectra (Figure 6) were simulated by the dmfit program.<sup>27</sup> The extracted NMR parameters are reported in Table 1. These parameters should provide information about the vanadium sites since relationships between NMR parameters and structural parameters were previously estab-

**Scheme 1. CrystalMaker Drawing of  $[\text{V}_{10}\text{O}_{28}]^{6-}$  Anion<sup>a</sup>**



<sup>a</sup> Black circles represent vanadium atoms, and gray circles represent oxygen atoms. One member of each set of symmetry equivalent vanadium atoms is labeled.

lished on model polyoxovanadate compounds.<sup>18–25</sup> These investigations were performed mainly on orthovanadates ( $\text{MVO}_4$ ), monovalent or divalent metal metavanadates ( $\text{MVO}_3$  and  $\text{M}(\text{VO}_3)_2$ ), and divalent metal pyrovanadates ( $\text{M}_2\text{V}_2\text{O}_7$ ). The  $^{51}\text{V}$  MAS NMR spectra consist of superimposed patterns of spinning sidebands extending over a spectral width of about 500 kHz and representing at least three sites. Indeed, the  $^{51}\text{V}$  NMR spectra display three resonances at around -560, -530, and -435 ppm whose distribution intensity varies significantly between the three samples. Therefore, this NMR study points out a striking difference in the chemical composition of the YF samples despite the fact that they were all prepared through an identical synthesis procedure. These samples contain the same polyoxovanadates species but their relative amount differs from one sample to the other. The chemical shifts of the three signals are different from those reported for crystalline  $\text{V}_2\text{O}_5$  (-620 ppm)<sup>36,37</sup> and  $\text{V}_2\text{O}_5\cdot n\text{H}_2\text{O}$  xerogels (-576, -596, -623, and -662 ppm).<sup>24,38</sup> The signal at -435 ppm may be assigned to a distorted  $\text{VO}_6$  site of a decavanadate anion since the  $^{51}\text{V}$  chemical shift ( $\delta_{\text{iso}}$ ), CSA ( $\Delta\delta_{\text{CSA}}$  and  $\eta_{\text{CSA}}$ ), and quadrupolar parameters ( $\eta_Q$ ) agree fairly well with those of the octahedral vanadium site at -427 ppm present in the  $\text{Cs}_4[\text{H}_2\text{V}_{10}\text{O}_{28}]\cdot 4\text{H}_2\text{O}$  compound (see Table 1). Taking into account the ideal symmetry of the decavanadate anion ( $mmm$ ), there are three non-equivalent  $\text{VO}_6$  octahedra showing a peculiar geometry (see Scheme 1). The vanadium site at -435 ppm corresponds to the central distorted octahedron (type 3) located in the equatorial plane of the polyanion. The quadrupole coupling parameter ( $C_Q$ ) for the site at -435 ppm is the only parameter that differs significantly from the value obtained for the  $\text{Cs}_4[\text{H}_2\text{V}_{10}\text{O}_{28}]\cdot 4\text{H}_2\text{O}$  compound. However, both values are quite large and reflect a vanadium site with a distorted electronic environment. Moreover since the spectrum consists of superimposed patterns of spinning sidebands representing

(36) Fontenot, C. J.; Wiench, J. W.; Schrader, G. L.; Pruski, M. *J. Am. Chem. Soc.* **2002**, *124*, 8435.

(37) Skibsted, J.; Nielsen, N. C.; Bildsoe, H.; Jakobsen, H. *J. Chem. Phys. Lett.* **1992**, *188*, 405.

(38) Durupthy, O.; Steunou, N.; Coradin, T.; Maquet, J.; Bonhomme, C.; Livage, J. *J. Mater. Chem.* **2005**, *15*, 1090.

up to three sites, its resolution is not high enough to allow an accurate determination of the quadrupole coupling parameters ( $C_Q$  and  $\eta_Q$ ). The  $^{51}\text{V}$  chemical shift ( $\delta_{\text{iso}}$ ), CSA ( $\Delta\delta_{\text{CSA}}$  and  $\eta_{\text{CSA}}$ ), and quadrupole coupling parameters ( $C_Q$  and  $\eta_Q$ ) of the signal at  $-530$  ppm are in good agreement with those obtained for the octahedral sites of  $\text{Cs}_4[\text{H}_2\text{V}_{10}\text{O}_{28}]\cdot 4\text{H}_2\text{O}$  at  $-518$ ,  $-531$ ,  $-540$ , and  $-545$  ppm (see Table 1). In particular, the value of the  $\Delta\delta_{\text{CSA}}$  parameter ( $-350$  ppm) indicates a strong distortion of the vanadium site. This signal corresponds to the distorted octahedral vanadium sites (types 1 and 2) present in the structure of the polyanion. In the case of the third sample (Figure 6b), this resonance is slightly shifted toward low field ( $-515$  ppm) which may be due to a possible protonation of these octahedral sites changing the  $^{51}\text{V}$  chemical shift.<sup>39,40</sup> Although the Hahn echo sequence is not suitable for a quantitative analysis, the resonance integration gives a 2:8 ratio between the two signals at  $-435$  and  $-530$  ppm in agreement with the decavanadate structure. The last signal at  $-564$  ppm has very low  $\Delta\delta_{\text{CSA}}$  ( $-140$  ppm) and  $\eta_{\text{CSA}}$  (0.2) values that are consistent with a tetrahedral vanadium site. The  $C_Q$  value of 2 MHz is also in good agreement with values proposed in the literature for such an environment.<sup>23</sup> From NMR data, it is possible to suggest whether the structure of the polyoxovanadate is made of infinite chains of condensed tetrahedrons (metal metavanadate  $\text{MVO}_3$ ) or of molecular oligomers (orthovanadate  $[\text{VO}_4]^{3-}$ , pyrovanadate  $[\text{V}_2\text{O}_7]^{4-}$ , or cyclic tetravanadate  $[\text{V}_4\text{O}_{12}]^{4-}$ ). Indeed, previous NMR studies showed that  $\Delta\delta_{\text{CSA}}$  and  $\eta_{\text{CSA}}$  parameters can be used to distinguish the polyoxovanadate with tetrahedrally coordinated  $\text{V}^{5+}$  (i.e.,  $0 < |\Delta\delta_{\text{CSA}}| < 100$  ppm for  $\text{VO}_4$  units in orthovanadate,  $60 \leq |\Delta\delta_{\text{CSA}}| \leq 260$  ppm for  $\text{VO}_4$  units in pyrovanadate,  $220 < |\Delta\delta_{\text{CSA}}| < 320$  ppm and  $0.65 \leq \eta_{\text{CSA}} \leq 0.80$  for  $\text{VO}_4$  units in monovalent metal metavanadate  $\text{MVO}_3$ ).<sup>19,22,23,25</sup> The  $|\Delta\delta_{\text{CSA}}|$  ranges indicate that the vanadium site at  $-564$  ppm cannot be assigned either to a  $\text{VO}_4$  site in orthovanadate or to a  $\text{VO}_4$  site in  $\text{MVO}_3$ . Furthermore, the  $\eta_{\text{CSA}}$  value is also significantly smaller than those typically observed for  $\text{MVO}_3$ .<sup>21</sup> Therefore, the signal at  $-564$  ppm may be assigned to molecular pyrovanadate  $[\text{V}_2\text{O}_7]^{4-}$  species. It might also correspond to other tetrahedral vanadate species such as the cyclic tetramers  $[\text{V}_4\text{O}_{12}]^{4-}$  ions. However, the lack of solid-state NMR characterization on  $[\text{V}_4\text{O}_{12}]^{4-}$  compounds prevents us from making unambiguous conclusions. These solid-state  $^{51}\text{V}$  NMR results show that the inorganic part of the yellow foams should be made of  $[\text{H}_x\text{V}_{10}\text{O}_{28}]^{(6-x)-}$  and  $[\text{V}_2\text{O}_7]^{4-}/[\text{V}_4\text{O}_{12}]^{4-}$  polyanions rather than a vanadium oxide network. The proportion of both species is varying from almost only  $[\text{V}_2\text{O}_7]^{4-}/[\text{V}_4\text{O}_{12}]^{4-}$  species (Figure 6a) to a large majority of  $[\text{H}_x\text{V}_{10}\text{O}_{28}]^{(6-x)-}$  ions (Figure 6c) depending widely on the sample.

**Reactivity of the YF.** The evolution of decavanadate, divanadate, and tetravanadate polyanions with pH is well-known in aqueous solution.<sup>41</sup> Therefore, by reacting the YF with acidic and basic gaseous phases, one can expect a

possible conversion of the polyanions constituting the YF by changing the pH, thereby confirming the proposed structure of the YF. Moreover, unexpected vanadium oxide structures and morphologies may be formed by this approach. In particular, acidification of the YF may favor the condensation of vanadium species within the foam walls.<sup>5</sup>

The reaction of the YF under vapors of aqueous ammonia led to a white compound (WF) that was stable with time in air. In contrast under vapors of hydrochloric acid, the YF transformed into a red compound (RF) that progressively evolved into a green compound (GF). The SEM pictures show that the macroscopic porosity observed in the initial YF does not remain in the modified WF and GF compounds. X-ray diffraction patterns of the modified foams (Figure 4b–d) are very similar to the one of the YF. They display the same  $00l$  series of reflections with a  $d_{001}$  value of 3.3 nm for WF and 3.0 nm for the RF and GF. This slight difference may be due to a difference in the packing of the hexadecylamine chains or the nature of the inorganic part. Thermogravimetric analyses of WF, RF, and GF are also very similar to that of the YF, showing that the amount of hexadecylamine and water are almost the same in the different foams. The modified foams were characterized by IR spectroscopy. The IR spectrum of the RFs could not be obtained because of their high instability with time in air. The vibration bands of the hexadecylamine in the modified foams WF and GF are almost identical to those of YF while those of the vanadium oxide network are quite different. The IR spectrum of WF display two vibrations bands at 920 and 960  $\text{cm}^{-1}$  that can be assigned to  $\nu(\text{V}=\text{O})$  vibrations. These vibrations are identical to those of YF. In contrast, the vibration  $\nu(\text{V}=\text{O})$  of GF is shifted to 1010  $\text{cm}^{-1}$ , which is identical to the vibration observed with a  $\text{V}_2\text{O}_5$  xerogel.<sup>42</sup> Actually, spectra of  $\text{V}_2\text{O}_5$  xerogels and GF exhibit also a broad vibration band between 500 and 600  $\text{cm}^{-1}$ , corresponding to the  $\nu(\text{V}_3\text{O})$  vibration of the vanadium oxide network.<sup>42</sup>

The color of the different foams is indicative of the amount of V(IV) species within the solid. WF are probably almost V(IV) free while RF may contain a few percent, and GF a yet larger amount. These observations can be confirmed by ESR experiments. The ESR spectra of the WF, YF, and RF are quite similar (Figure 5a–c). The main difference arises from the line width of the signal that increases from WF to RF. This is consistent with an increase of the V(IV) rate from WF to RF. It becomes quite large in the green foams where the hyperfine structure is no longer resolved leading to a single broad signal (Figure 5d). This evolution from ESR spectra with an hyperfine structure (ESR spectrum of WF or YF) to ESR spectra dominated by a single signal (ESR spectrum of GF) is similar to the evolution observed for  $\text{V}_2\text{O}_5$  xerogels with an increasing amount of V(IV) ions between 1 and 16%.<sup>43</sup> On the basis of these experiments, one can expect that the V(IV) rate is presumably smaller than 3% in WF and YF, larger in RF, and may reach a value close to

(39) Howarth, O. W. *Prog. Nucl. Magn. Reson. Spectrosc.* **1990**, 22, 453.

(40) Heath, E.; Howarth, O. W. *J. Chem. Soc., Dalton Trans.* **1981**, 1105.

(41) Baess, C. F.; Mesmer, R. E., *Hydrolysis of Cations*; Wiley: New York, 1976.

(42) Abello, L.; Husson, E.; Repelin, Y.; Lucazeau, G. *J. Solid State Chem.* **1985**, 56, 379.

(43) Babonneau, F.; Barboux, P.; Josien, F. A.; Livage, J. *J. Chim. Phys.* **1985**, 82, 761.

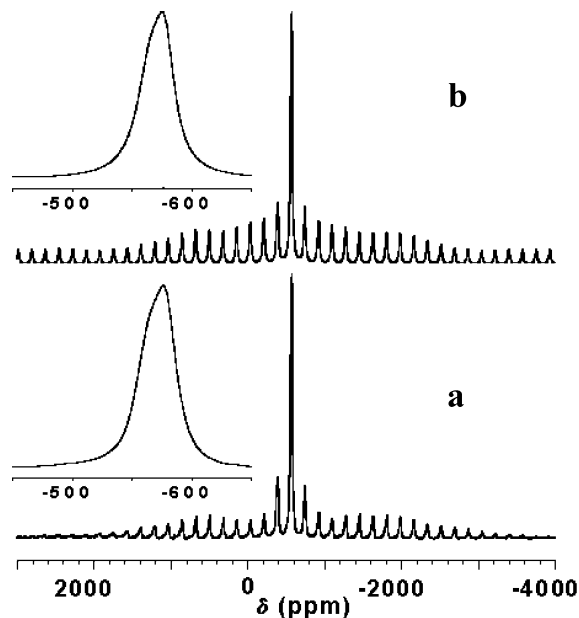


**Figure 7.** (a)  $^{51}\text{V}$  MAS NMR spectrum of WF. (b) Simulation performed with QUASAR. The isotropic part of the spectra is enlarged in the inset.

15% in GF. Since the amount of V(IV) does not presumably exceed 15% in the different foams, these compounds were characterized by  $^{51}\text{V}$  MAS NMR spectroscopy. The experimental and simulated  $^{51}\text{V}$  MAS NMR spectra of the white foam are shown in Figure 7. The spinning sidebands can be observed over a range of 500 kHz. The most intense peak that corresponds to the isotropic part of the spectrum was simulated with two different signals at  $-578$  and  $-564$  ppm. The set of parameters obtained are listed in Table 1. Signals corresponding to the decavanadate species in the pristine YF are no longer observed, in agreement with the dissociation of those ions above pH 7.<sup>40,41</sup> The white color of the foams is also in agreement with the absence of orange-yellow decavanadate species. The signal at  $-564$  ppm corresponds to the already described signal of the YF with similar CSA and quadrupole coupling parameters. The signal at  $-578$  ppm exhibits also a low  $\Delta\delta_{\text{CSA}}$  ( $-200$  ppm) and  $\eta_{\text{CSA}}$  (0.3) values consistent with a tetrahedrally coordinated  $\text{V}^{5+}$ . According to  $\Delta\delta_{\text{CSA}}$  and  $\eta_{\text{CSA}}$  values range reported previously,<sup>19,22,23,25</sup> this last signal may correspond to pyrovanadate ions ( $60 \leq |\Delta\delta_{\text{CSA}}| \leq 260$  ppm) rather than metavanadate chains  $\text{MVO}_3$  that exhibit larger  $|\Delta\delta_{\text{CSA}}|$  (i.e.,  $|\Delta\delta_{\text{CSA}}| > 220$  ppm) and  $\eta_{\text{CSA}}$  values (i.e.,  $0.65 \leq \eta_{\text{CSA}} \leq 0.80$ ).<sup>19,22,23,25</sup> This result is also in good agreement with the chemistry of vanadium in solution: at  $9 < \text{pH} < 13$  values, pyrovanadate  $[\text{V}_2\text{O}_7]^{4-}$  ions are among the predominating polyoxovanadate species.

$^{51}\text{V}$  MAS NMR experiments of the RFs were performed as follows. YFs were acidified with HCl vapors for 10 min and then left to dry 2 h in air. The sample was then packed in a 4 mm  $\text{ZrO}_2$  rotor, and successive acquisitions of 14 000 transients were performed every 2 h up to 18 h in order to follow the conversion of the RF into GF. The  $^{51}\text{V}$  MAS NMR spectra could not be fitted due to the presence of V(IV) paramagnetic centers in the acidified foams, a short acquisition time, and a high number of different signals as well. The spectra display a broad isotropic peak, which can be

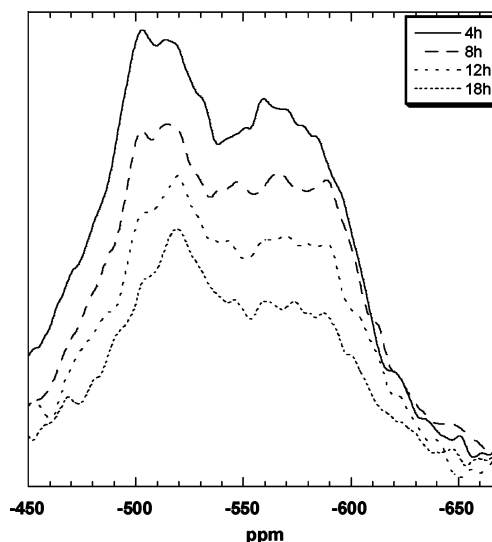


**Figure 8.** Isotropic part of the  $^{51}\text{V}$  MAS NMR spectrum of RF, 4 h (—), 8 h (---), 12 h (···), and 18 h (— · —) after acidification. All the spectra were recorded in the same conditions and with the same scan number (NS = 14000).

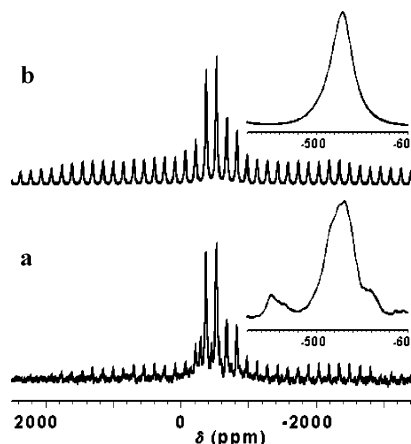
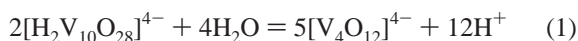


**Figure 9.**  $^{51}\text{V}$  MAS NMR spectrum of the GF. (b) Simulation of the main signal performed with QUASAR. The isotropic part of the spectra is enlarged in the inset.

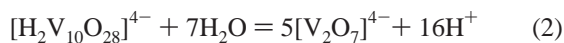
divided into two different chemical shift regions (see Figure 8). The region between  $-450$  and  $-540$  ppm may be assigned to decavanadate species that are conserved from the pristine product. The broad peak between  $-560$  and  $-600$  ppm is the typical chemical shift range where resonances of a  $\text{V}_2\text{O}_5$  xerogel can be observed.<sup>24,38</sup> Actually, four different sites of a  $\text{V}_2\text{O}_5 \cdot 1.5 \text{H}_2\text{O}$  xerogel give rise to signals at  $-663$ ,  $-623$ ,  $-596$ , and  $-576$  ppm. Moreover the red color of the foam and the acidic conditions are consistent with the formation of a xerogel and the presence of decavanadate species. A global decrease of the signal intensity can be observed with time and is mainly due to the increasing rate of V(IV) in the foam. However, a signal at  $-520$  ppm in the decavanadate region seems unaffected. This signal cannot be unambiguously assigned from these experiments. Therefore, another  $^{51}\text{V}$  MAS NMR spectrum of GF aged for 1 month was recorded. Figure 9 displays the experimental  $^{51}\text{V}$  MAS NMR spectrum and the simulation of the main signal at  $-525$  ppm (two small signals at  $-450$  and  $-560$  ppm were also observed but could not be simulated). The corresponding NMR parameters of the signal

at  $-525$  ppm are reported in Table 1. The value of  $\Delta\delta_{\text{CSA}}$  ( $-350$  ppm) is larger than those commonly observed for tetrahedrally coordinated  $\text{V}^{5+}$  ( $|\Delta\delta_{\text{CSA}}| > 300$  ppm).<sup>19,22,23,25</sup> This means that this vanadium site may exhibit a distorted  $\text{VO}_5$  or  $\text{VO}_6$  symmetry. However, the  $\Delta\delta_{\text{CSA}}$  value of the site at  $-525$  ppm is also significantly smaller than those reported for distorted octahedral environments such as in  $\text{V}_2\text{O}_5 \cdot n\text{H}_2\text{O}$  xerogels.<sup>24,38</sup> Therefore, this site may possess a trigonal bipyramidal or a square pyramidal environment. The  $^{51}\text{V}$  chemical shift ( $\delta_{\text{iso}}$ ), CSA ( $\Delta\delta_{\text{CSA}}$ ), and quadrupolar parameters ( $C_Q$  and  $\eta_Q$ ) are in good agreement with those of the trigonal bipyramidal site ( $\text{V}_a$ ) reported previously for the  $\text{NaV}_3\text{O}_8 \cdot 1.5 \text{H}_2\text{O}$  compound (see Table 1).<sup>38</sup>

**Formation of the Vanadium Oxide Foams.** The dissolution of  $\text{V}_2\text{O}_5$  in an aqueous solution of hydrogen peroxide is commonly used for the preparation of  $\text{V}_2\text{O}_5 \cdot n\text{H}_2\text{O}$  gels. This reaction leads first to the complexation of vanadium by the peroxy ligands as evidenced by solution  $^{51}\text{V}$  NMR.<sup>44,45</sup> Then the exothermic decomposition of peroxy groups with an important release of oxygen gas gives rise to a vanadate solution of pH 2 containing a mixture of decavanadate  $[\text{H}_2\text{V}_{10}\text{O}_{28}]^{4-}$  and  $[\text{VO}_2]^+$  ions.<sup>44</sup> The introduction of amines in the solution together with  $\text{V}_2\text{O}_5$  and  $\text{H}_2\text{O}_2$  provokes a modification of the composition and the reactivity of the reaction medium. First, in the presence of amines, the pH of the solution is expected to be higher than 2. However, a pH value of 2 was measured when the formation of the foam started, which means that the solution is composed mainly of  $[\text{VO}_2]^+$  and  $[\text{H}_2\text{V}_{10}\text{O}_{28}]^{4-}$  ions. Furthermore, since the decomposition of hydrogen peroxide is strongly exothermic, the subsequent increase of temperature up to  $60$  °C may lead to a modification of the equilibrium between polyoxovanadates. Indeed, it was previously observed by  $^{51}\text{V}$  NMR spectroscopy in solution that an equilibrium between  $[\text{H}_2\text{V}_{10}\text{O}_{28}]^{4-}$  and  $[\text{V}_4\text{O}_{12}]^{4-}$  at pH 7 can be progressively displaced toward the formation of  $[\text{V}_4\text{O}_{12}]^{4-}$  when the temperature increases (eq 1):<sup>46</sup>

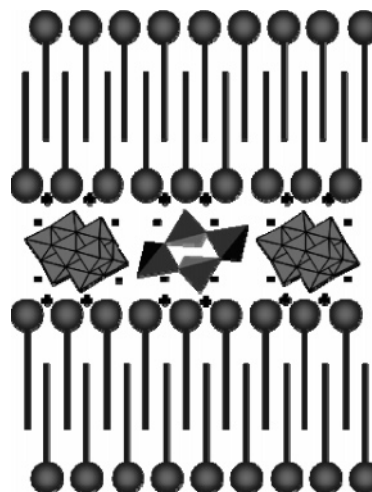


We can hypothesize that a similar conversion of  $[\text{H}_2\text{V}_{10}\text{O}_{28}]^{4-}$  into  $[\text{V}_2\text{O}_7]^{4-}$  may occur as



Therefore, the increase of the temperature in the reaction medium may lead to the formation of  $[\text{H}_x\text{V}_{10}\text{O}_{28}]^{(6-x)-}$  and  $[\text{V}_4\text{O}_{12}]^{4-}$  ions that precipitate into the inorganic phase constituting the foam walls. No polycondensation of vanadium was observed during this foaming process although a vanadate solution of pH 2 usually turns to a red  $\text{V}_2\text{O}_5 \cdot n\text{H}_2\text{O}$  gel after about 12–24 h depending on the concentration of vanadium. At pH 2, it was suggested previously that decavanadate ions could behave as a reservoir of  $\text{V}^{\text{V}}$  precursors that condense into the vanadium oxide net-

**Scheme 2. Proposed Chemical Structure of the Yellow Foam (YF)**



work.<sup>38,47</sup> The absence of any vanadium polycondensation may be due in part to the amphiphilic character of the hexadecylamines. Indeed, it is well-known that surfactant molecules self-organize in solution into stable aggregates with interfacial properties that favor a stabilization and a compatibility of media with different cohesion energies or their partition. The self-assembly of hexadecylamine molecules in aqueous solution can result in aggregates like micelles or continuous morphologies like cylinders or lamellae. Therefore, the structure of the vanadium oxide foam may be based on the packing of vanadium oxide polyanions and amine assemblies. Indeed, the structure of a vanadium oxide–dodecylamine hybrid compound was previously determined.<sup>48</sup> This compound exhibits a lamellar phase which consists of discrete decavanadate clusters, between which the lamellar assemblies of cationic surfactant reside. The negative charge of the polyanions is balanced by the protonated ammonium headgroup of surfactants. The clusters are joined by hydrogen bonds from water molecules. A strong dehydration of the crystals was observed, which made difficult the acquisition of the X-ray data.<sup>48</sup> This dehydration should be inherent to the lamellar assemblies of amines in the structure which are rather prone to solubilize hydrophobic compound. Similarly, almost no water is present in the vanadium oxide foams. Therefore, we can suggest that the YF exhibits a structure based on layers of amines between which  $[\text{H}_x\text{V}_{10}\text{O}_{28}]^{(6-x)-}$  and  $[\text{V}_4\text{O}_{10}]^{4-}/[\text{V}_2\text{O}_7]^{4-}$  polyanions are inserted (see Scheme 2). This structure may be compared to the one observed for polyoxometalates intercalated between the positively charged layers of long alkylammonium chains in Langmuir–Blodgett films.<sup>49–51</sup> In this proposed model, the stability of the foam walls results from electrostatic interactions between the negatively charged  $[\text{H}_x\text{V}_{10}\text{O}_{28}]^{(6-x)-}$  and  $[\text{V}_4\text{O}_{10}]^{4-}/[\text{V}_2\text{O}_7]^{4-}$  polyanions and the

(44) Alonso, B.; Livage, J. *J. Solid State Chem.* **1999**, *148*, 16.

(45) Fontenot, C. J.; Wiench, J. W.; Pruski, M.; Schrader, G. L. *J. Phys. Chem. B* **2000**, *104*, 11622.

(46) Bouhedja, L.; Steunou, N.; Maquet, J.; Livage, J. *J. Solid State Chem.* **2001**, *162*, 315.

(47) Pozarnsky, G. A.; McCormick, A. V. *Chem. Mater.* **1994**, *6*, 380.

(48) Janauer, G. G.; Doble, A. D.; Zavalij, P. Y.; Whittingham, M. S. *Chem. Mater.* **1997**, *9*, 647.

(49) Clemente-Leon, M.; Mingotaud, C.; Gomez-Garcia, C. J.; Coronado, E.; Delhaes, P. *Thin Solid Films* **1998**, *327–329*, 439.

(50) Liu, S.; Tang, Z.; Wang, E.; Dong, S. *Thin Solid Films* **1999**, *339*, 277.

(51) Zhong, L.-F.; Zhang, Y.-M.; Tang, Y.; Bai, Y. *Polyhedron* **2003**, *22*, 2647.

positively charged head of the resulting alkylammonium. We may assume that the dehydration of the vanadium oxide foams is strongly favored by a temperature of 60 °C and by the presence of large bubbles in the reaction medium. Therefore, this strong water evaporation prevents any vanadium polycondensation and may induce the self-assembly of amines into lamellae structures. A self-assembly of surfactants assisted by the solvent evaporation was previously reported for the preparation of mesoporous silica or transition metal oxide thin films.<sup>52–55</sup>

The reaction of the yellow foams with basic or acidic vapors is in good agreement with the composition of the YF. Indeed,  $[\text{H}_x\text{V}_{10}\text{O}_{28}]^{(6-x)-}$  and  $[\text{V}_4\text{O}_{10}]^{4-}/[\text{V}_2\text{O}_7]^{4-}$  polyanions in YF walls exhibit the same reactivity in the foams than in aqueous solution by varying the pH. The basic treatment of the YF leads to a white compound. <sup>51</sup>V NMR spectroscopy confirms that this WF is made of tetrahedral vanadate species such as  $[\text{V}_4\text{O}_{10}]^{4-}$  and/or  $[\text{V}_2\text{O}_7]^{4-}$  ions that are among the predominant vanadate species at basic pH.<sup>41</sup> Therefore, the conversion under basic conditions of  $[\text{H}_x\text{V}_{10}\text{O}_{28}]^{(6-x)-}$  into  $[\text{V}_4\text{O}_{10}]^{4-}/[\text{V}_2\text{O}_7]^{4-}$  may take place according to eqs 1 and 2. A condensation of vanadium expected at low pH is currently observed after the exposure of the YF to HCl vapors. The resulting RFs consist of decavanadate species and condensed  $\text{V}_2\text{O}_5$  layers as evidenced by <sup>51</sup>V MAS NMR spectroscopy. Such a condensation process within surfactant wall via the reaction with a gaseous phase has already been used for the synthesis of PbS particles in Langmuir–Blodgett films.<sup>56</sup> This RF was not stable with time and turns to green, suggesting the reduction of a large amount of V(IV) centers. This reduction enhanced under acidic conditions may be due to the larger

value at low pH of the  $\text{V}^{5+}/\text{V}^{4+}$  potential ( $E^\circ = 1.0\text{--}0.12$  pH)<sup>57</sup> as compared to the one of  $\text{Cl}_2/\text{Cl}^-$  ( $E^\circ = 1.36$  V).<sup>57</sup> The presence of a large amount of V(IV) species in this probably condensed inorganic lattice prevents us from proposing a structure of the GF from either ESR or NMR. The poorly crystalline system cannot be determined either by diffraction. We may only suggest that the transformation of RF into GF results from a structural rearrangement of the vanadium oxide network and the partial reduction of the vanadium (V).

## Conclusions

Despite the disordered nature of the vanadium oxide foams, the identification of the polyoxovanadates constituting the YF is rendered possible by solid-state <sup>51</sup>V NMR. These experiments allow the determination of the CSA and quadrupole coupling parameters that can be correlated with the geometry of the vanadium sites. The CSA ( $\Delta\delta_{\text{CSA}}$  and  $\eta_{\text{CSA}}$ ) parameters are especially useful in distinguishing the tetrahedral from octahedral vanadium sites in YF. A comparison of the CSA and quadrupole coupling parameters with reference compounds suggests that YF are made of molecular  $[\text{H}_x\text{V}_{10}\text{O}_{28}]^{(6-x)-}$  and  $[\text{V}_4\text{O}_{10}]^{4-}/[\text{V}_2\text{O}_7]^{4-}$  polyanions. The relative amount of the different polyoxovanadate species could not be controlled due to the high reactivity of  $\text{V}_2\text{O}_5$  with  $\text{H}_2\text{O}_2$ . The possible formation of a condensed lamellar vanadium oxide like  $\text{V}_2\text{O}_5$  at pH 2 can be ruled out from these NMR experiments. Therefore, the layered structure of the YF evidenced by X-ray diffraction can rather arise from a self-assembly of the amines into layers between which  $[\text{H}_x\text{V}_{10}\text{O}_{28}]^{(6-x)-}$  and  $[\text{V}_4\text{O}_{10}]^{4-}/[\text{V}_2\text{O}_7]^{4-}$  polyanions are intercalated. The identification of the polyoxovanadates constituting the WF and RF compounds by <sup>51</sup>V MAS NMR is in fair agreement with the reactivity in aqueous solution of  $[\text{H}_x\text{V}_{10}\text{O}_{28}]^{(6-x)-}$  and  $[\text{V}_4\text{O}_{10}]^{4-}/[\text{V}_2\text{O}_7]^{4-}$  polyanions by changing pH.

CM051429Y

- (52) Doshi, D. A.; Gibaud, A.; Goletto, V.; Lu, M.; Gerung, H.; Ocko, B.; Han, S. M.; Brinker, C. J. *J. Am. Chem. Soc.* **2003**, *125*, 11646.  
 (53) Lu, Y.; Fan, H.; Doke, N.; Loy, D. A.; Assink, R. A.; LaVan, D. A.; Brinker, C. J. *J. Am. Chem. Soc.* **2000**, *122*, 5258.  
 (54) Grosso, D.; Cagnol, F.; Soler-Illia, G. J. D. A. A.; Crepaldi, E. L.; Amenitsch, H.; Brunet-Bruneau, A.; Bourgeois, A.; Sanchez, C. *Adv. Funct. Mater.* **2004**, *14*, 309.  
 (55) Crepaldi, E. L.; Soler-Illia, G. J. d. A. A.; Grosso, D.; Cagnol, F.; Ribot, F.; Sanchez, C. *J. Am. Chem. Soc.* **2003**, *125*, 9770.  
 (56) Li, L. S.; Qu, L.; Wang, L.; Lu, R.; Peng, X.; Zhao, Y.; Li, T. J. *Langmuir* **1997**, *13*, 6183.

- (57) Pourbaix, M.; Deltombe, E.; Zoubov, N., *Atlas d'équilibres électrochimiques*; Gauthier-Villars: Paris, 1963.